

# Key role of continental margin sediments in the oceanic mass balance of Zn and Zn isotopes

**Journal Article****Author(s):**

Little, Susan H.; Vance, Derek; McManus, James; Severmann, Silke

**Publication date:**

2016-03

**Permanent link:**

<https://doi.org/10.3929/ethz-b-000113977>

**Rights / license:**

[In Copyright - Non-Commercial Use Permitted](#)

**Originally published in:**

Geology 44(3), <https://doi.org/10.1130/g37493.1>

1 Key role of continental margin sediments in the oceanic  
2 mass balance of Zn and Zn isotopes

3 Susan H. Little<sup>1,2</sup>, Derek Vance<sup>2</sup>, James McManus<sup>3</sup>, and Silke Severmann<sup>4</sup>

4 <sup>1</sup>*Department of Earth Science and Engineering, Imperial College London, London SW7*  
5 *2BP, UK*

6 <sup>2</sup>*Institute of Geochemistry and Petrology, Department of Earth Sciences, ETH Zürich,*  
7 *8092 Zürich, Switzerland*

8 <sup>3</sup>*Department of Geosciences, University of Akron, Akron, Ohio 44325-4101, USA*

9 <sup>4</sup>*Department of Marine & Coastal Science, Rutgers, The State University of New Jersey,*  
10 *New Brunswick, NJ 08901-8521, USA*

11 **ABSTRACT**

12 Zinc is an essential micronutrient and its concentration and isotopic composition  
13 in marine sediments represent promising tracers of the ocean carbon cycle. However,  
14 gaps remain in our understanding of the modern marine cycle of Zn, including an  
15 explanation of the heavy Zn isotopic composition of seawater relative to the known  
16 inputs, and the identity of a required ‘missing sink’ for light Zn isotopes. Here we present  
17 Zn isotope data for organic- and trace metal-rich continental margin sediments from the  
18 east Pacific margins, which together provide the first observational evidence for the  
19 previously hypothesized burial of light Zn in such settings. In turn, this light Zn output  
20 flux provides a means to enrich the seawater dissolved pool in heavy isotopes. The size  
21 and isotopic composition of the margin sink is controlled by the uptake of Zn into organic  
22 matter in the photic zone and the fixation of this pool, probably in the form of Zn-

23 sulfides, in sediments. An estimate of its significance to the overall Zn oceanic mass  
24 balance, both in terms of flux and isotopic composition, indicates that such settings can  
25 fulfill the requirements of the missing Zn sink. Taken together, these observations have  
26 important implications for the interpretation of Zn isotope data for marine sediments in  
27 the geologic record.

## 28 **INTRODUCTION**

29 Zinc is utilized in almost 100 Zn-specific enzymes across all five kingdoms of life  
30 (U.S. NRC, 2000). Its significance in the oceanic realm stems primarily from its role as a  
31 cofactor in two key enzymes: carbonic anhydrase, involved in carbon fixation, and  
32 alkaline phosphatase, active in phosphorus uptake and cycling (Sinoir et al., 2012). Under  
33 certain conditions, Zn may limit primary production (Morel et al., 1994). Its importance  
34 as a micronutrient, combined with procedural and analytical advances and the sampling  
35 capacity of the GEOTRACES program (SCOR Working Group, 2007), has motivated a  
36 new generation of studies of the modern oceanic cycling of Zn and its isotopes (e.g.,  
37 Little et al., 2014; Zhao et al. 2014; Conway and John, 2014; John and Conway, 2014;  
38 Roshan and Wu, 2015; Janssen and Cullen, 2015).

39 Zinc isotopes offer insight both into the processes controlling water column Zn  
40 distributions, and constraints on its global oceanic mass balance. Furthermore, the likely  
41 strong biological control on dissolved Zn availability has motivated the use of  $\delta^{66}\text{Zn}$  as a  
42 tracer of past ocean productivity (Kunzmann et al., 2012). However, there remains a  
43 considerable gap in our understanding of the modern Zn oceanic mass balance (Little et  
44 al., 2014), which limits our interpretation of paleo-Zn isotope data. An isotopically light  
45 sink is required both to balance the marine Zn budget, and to explain the isotopically

46 heavy composition of dissolved Zn in the modern ocean with respect to the primary Zn  
47 inputs (seawater ~0.5‰; cf. rivers, dust, hydrothermal fluids and sediments, all  $\leq$ 0.3‰;  
48 see Fig. 1). In this study we present new Zn isotope data for organic-rich sediments from  
49 several oxygen-deficient sites along the east Pacific margin. These data provide the first  
50 observational evidence of a hypothesized light sink for Zn buried in organic-rich  
51 sediments (Little et al., 2014; Zhao et al., 2014).

## 52 **SITES AND SAMPLING**

53 We studied samples from well-characterized sites from the north- and south-  
54 eastern Pacific margin (Table 1, Fig. DR1). They include four California borderland  
55 basins (Santa Barbara, Santa Monica, San Nicolas and Tanner Basins), three sites from  
56 along the Mexican margin (Magdalena, Soledad Basin and Pescadero slope), and one site  
57 at the center of the intense oxygen minimum zone (OMZ) along the Peru margin. All  
58 three margins are slope-dominated, characterized by upwelling-driven productivity.  
59 Taken together, they encompass a range of reducing (low oxygen) conditions and  
60 diagenetic environments found along an open ocean margin (Table 1).

61 Sediment cores were collected using a multi-corer as described previously  
62 (McManus et al., 2006). Cores from the Mexico and Peru margins have low bottom water  
63 oxygen concentrations and cover a range of diagenetic regimes from ferruginous to  
64 sulfidic (Table 1, McManus et al., 2006; Chong et al., 2012). The borderland basins have  
65 a broader range in bottom water oxygen contents and include settings that are typically  
66 manganeseous to ferruginous (Table 1).

## 67 **ANALYTICAL METHODS**

68 For bulk concentration and isotope measurements, 100–500 mg of powdered  
69 sediment was treated with dilute nitric acid to dissolve carbonate, digested in a 3:1 mix of  
70 concentrated HF and HNO<sub>3</sub>, and treated three times with concentrated HNO<sub>3</sub> to re-  
71 dissolve fluoride salts before final dissolution in 7M HCl. An aliquot of the total digest  
72 solutions was taken for elemental analysis on a Thermo Element 2 at the University of  
73 Bristol or ETH Zürich (for accuracy and precision data, see Little et al. (2014, 2015)).  
74 For isotope analysis, further aliquots were spiked with a <sup>64</sup>Zn-<sup>67</sup>Zn double spike to  
75 achieve sample-spike ratios of close to unity (Bermin et al., 2006). These Zn fractions  
76 were purified via anion exchange (Bermin et al., 2006) and analyzed on a Neptune  
77 (Bristol) or Neptune Plus (ETH) MC-ICP-MS using previously published protocols  
78 (Archer and Vance, 2004; Little et al., 2014). Two-sigma external reproducibility on  
79 δ<sup>66</sup>Zn analyses was estimated via double spike analysis of a secondary isotope standard,  
80 IRMM 3702, which gave δ<sup>66</sup>Zn = 0.30 ± 0.06‰ relative to Lyons-JMC (n = 163 over 24  
81 months). Other uncertainties are given as 2SD unless stated.

82 Organic carbon data are calculated as the difference between total carbon and  
83 inorganic carbon. Total carbon and sulfur were analyzed on a PerkinElmer Series 11  
84 CNHSO Analyzer, and inorganic carbon was measured on a UCI Inc. Coulometrics  
85 CMS130 Coulometer.

## 86 RESULTS

87 No analytically discernable depth dependent variation in bulk sediment δ<sup>66</sup>Zn  
88 values was observed for the sites we sampled (Fig. 2). δ<sup>66</sup>Zn<sub>bulk</sub> in the California and  
89 Mexican margin sites were consistently lighter than the lithogenic average (0.27 ± 0.07‰  
90 (1SD); Fig. 1, Table DR1), at –0.05–0.15‰. No resolvable isotopic variation was

91 observed among the California Borderland basins ( $0.11 \pm 0.08\text{‰}$ ), which together  
92 encompass a broad range in bottom water oxygen conditions (Table 1). Of the Mexican  
93 margin sites, the Magdalena margin site is distinct, exhibiting greater Zn enrichment  
94 reflected in higher Zn/Al values (by mass, expressed as ppm/wt%) and a slightly heavier  
95  $\delta^{66}\text{Zn}_{\text{bulk}}$  than the Pescadero slope and Soledad basin (Magdalena:  $0.12 \pm 0.02\text{‰}$ , cf.  
96 Soledad/Pescadero:  $0.01 \pm 0.06\text{‰}$ ). The Magdalena site represents an open ocean,  
97 unrestricted margin (Table 1). In this regard, it most closely resembles the Peru margin  
98 site, where mean  $\delta^{66}\text{Zn}_{\text{bulk}}$  is significantly different and isotopically heavier, at  $0.32 \pm$   
99  $0.06\text{‰}$ .

## 100 **DISCUSSION**

### 101 **Lithogenic versus ‘Bioauthigenic’ Zn**

102 Evaluation of the Zn flux from seawater into margin sediments requires a  
103 correction for the lithogenic (terrigenous) component of the sediment. Zinc is present at  
104  $\sim 70$  ppm in upper continental crust (Rudnick and Gao, 2003) and often at higher  
105 concentrations in shale (Wedepohl, 1991). The correction is made by assuming a  
106 homogenous Zn/Al ratio and isotopic composition of the lithogenic component,  
107  $(\text{Zn}/\text{Al})_{\text{lith}}$  and  $\delta^{66}\text{Zn}_{\text{lith}}$ , and using the measured Al concentration of the sample ( $\text{Al}_{\text{sample}}$ )  
108 as a tracer of the terrigenous component, to calculate its lithogenic Zn fraction ( $X_{\text{lith}}$ ) as  
109 follows:

$$110 \quad X_{\text{lith}} = ((\text{Zn}/\text{Al})_{\text{lith}} \times \text{Al}_{\text{sample}}) / \text{Zn}_{\text{sample}} \quad (1)$$

111 where  $\text{Zn}_{\text{sample}}$  is the total Zn concentration of the sample. The non-lithogenic, or  
112 ‘bioauthigenic’ component of the sediment,  $X_{\text{auth}}$ , which includes both authigenic

113 (chemically precipitated) and biogenic (cellular and/or skeletal) Zn, can then be simply  
114 calculated:

$$115 \quad X_{\text{auth}} = 1 - X_{\text{lith}}, \quad (2)$$

116 The isotope ratio of this bioauthigenic Zn fraction can then be calculated as  
117 follows:

$$118 \quad \delta^{66}\text{Zn}_{\text{auth}} = (\delta^{66}\text{Zn}_{\text{bulk}} - \delta^{66}\text{Zn}_{\text{lith}} \times X_{\text{lith}}) / X_{\text{auth}} \quad (3)$$

119 where  $\delta^{66}\text{Zn}_{\text{bulk}}$  is the measured isotope value of the sample. Finally, the  
120 bioauthigenic or ‘excess’ Zn concentration,  $\text{Zn}_{\text{XS}}$ , can be calculated:

$$121 \quad \text{Zn}_{\text{XS}} = \text{Zn}_{\text{sample}} - \text{Al}_{\text{sample}} \times (\text{Zn}/\text{Al})_{\text{lith}}. \quad (4)$$

122 In the absence of measurements of local lithogenic materials from the east Pacific  
123 margin we use global average lithogenic values. The isotopic composition of lithogenic  
124 Zn ( $\delta^{66}\text{Zn}_{\text{lith}}$ ) is  $0.27 \pm 0.07\text{‰}$  (1SD,  $n = 50$ , Figure 1, Table DR1). We assume a Zn/Al  
125 ratio of  $8.4 \times 10^{-4}$  (the most recent upper continental crust estimate; Rudnick and Gao,  
126 2003), and assign it a 1SD uncertainty of  $\pm 1 \times 10^{-4}$ . We then use a Monte-Carlo  
127 approach to evaluate the uncertainties on calculated  $\delta^{66}\text{Zn}_{\text{auth}}$  values. The uncertain  
128 variables ( $(\text{Zn}/\text{Al})_{\text{lith}}$ ,  $\delta^{66}\text{Zn}_{\text{lith}}$ , and  $\delta^{66}\text{Zn}_{\text{bulk}}$ ) were forced within their assigned  
129 uncertainties (1SDs of 1, 0.07‰, and 0.03‰ respectively) using normally-distributed  
130 pseudo-random numbers, and the  $\delta^{66}\text{Zn}_{\text{auth}}$  calculation performed 100,000 times.  $\delta^{66}\text{Zn}_{\text{auth}}$   
131 values for each sample and site were then calculated as the mean and 2SD of these  
132 100,000 iterations (Table DR2). The lithogenic correction is most significant and has a  
133 larger associated uncertainty for those samples with a high  $X_{\text{lith}}$  fraction and/or a large  
134 difference between  $\delta^{66}\text{Zn}_{\text{lith}}$  and  $\delta^{66}\text{Zn}_{\text{bulk}}$  (Figs. DR1, DR2). Nevertheless, strikingly light  
135  $\delta^{66}\text{Zn}_{\text{auth}}$  values are calculated for several of the sites, with values as low as  $-0.40 \pm$

136 0.37‰ (Pescadero slope, Table DR2). The validity of these calculated values remains to  
137 be tested, for example, through targeted sequential leaching of the non-lithogenic Zn  
138 pool.

### 139 **Margin Sediments: An Important Sink for Light Zn Isotopes**

140 The principal finding of this study is the presence of an isotopically light Zn  
141 fraction in oxygen-poor, organic-rich margin sediments (Fig. 3). The presence of this  
142 light Zn is likely the result of one or a combination of two processes: (1) biological  
143 uptake or (2) authigenic mineral precipitation.

144 Biological uptake may be accompanied by the preferential incorporation of light  
145 Zn isotopes by phytoplankton (John et al., 2007) and this signature may be preserved in  
146 the resultant organic-rich sediment. An apparent correlation of  $\delta^{66}\text{Zn}_{\text{auth}}$  with  $C_{\text{org}}$  content  
147 (Fig. 3a) may hint at such a surface ocean (uptake) control. However, a similar pattern  
148 emerges for  $\delta^{66}\text{Zn}_{\text{auth}}$  plotted versus total S (Fig. 3b), and there is no simple relationship  
149 between  $\delta^{66}\text{Zn}_{\text{auth}}$  and Zn/Al (Fig. 2), suggesting that the processes contributing to  
150  $\delta^{66}\text{Zn}_{\text{auth}}$  are complex. Despite evidence for biological Zn isotope fractionation in cultures  
151 (John et al., 2007), a biological, kinetic isotope effect is rarely evident in recent upper  
152 ocean water column data, particularly in micronutrient-limited regimes like the Southern  
153 Ocean (Zhao et al., 2014). Scavenging of Zn by particulate matter has instead been  
154 proposed to explain upper water column Zn isotope distributions (John and Conway,  
155 2014). Scavenging favors the heavy Zn isotope (John and Conway, 2014), however, and  
156 cannot be invoked to explain the light signature in margin sediments.

157 Alternatively, isotopic fractionation of Zn may occur during authigenic mineral  
158 precipitation, associated with the breakdown of, or desorption from, the carrier phase.



159 One such plausible mechanism is the precipitation of isotopically light authigenic ZnS  
160 phases (e.g., Fujii et al., 2011). Authigenic ZnS precipitation has been proposed to occur  
161 under certain conditions in the water column, associated with reducing  
162 microenvironments around biogenic particles (Conway and John, 2015; Janssen and  
163 Cullen, 2015). In other locations, contingent upon the location of redox fronts, ZnS  
164 precipitation may occur in sediments. Irrespective of the locus of sulfide precipitation, a  
165 corresponding heavy pool of dissolved Zn would be generated in the deep water or  
166 surface sediments, consistent with the observed isotopically heavy global seawater  
167 composition ( $\sim 0.5\%$ ). Apparently contrary to this view, however, light dissolved  $\delta^{66}\text{Zn}$   
168 values and elevated Zn concentrations have been observed in the water column along  
169 both continental margins in the North Atlantic as well as in the oxygen-poor San Pedro  
170 Basin off California (Conway and John, 2014; 2015). Neither Atlantic margin is strongly  
171 reducing, thus this data is not likely to be relevant to the sulfidization hypothesis.  
172 Conway and John (2015) explain light Zn in the San Pedro basin either through release of  
173 biogenic Zn, or redissolution of (water column) colloidal sulfide particles on periodic  
174 flushing of the deep basin with oxygenated water. While the latter may be consistent with  
175 the predictions in this study, further clarity awaits renewed efforts to obtain reliable Zn  
176 porewater data from similar settings.

177 We hypothesize that the markedly heavier Zn isotopic composition at the Peru  
178 margin site reflects near-complete (quantitative) Zn uptake from surface waters with a  
179 local isotopic composition distinctly lighter than the global average, as is observed in the  
180 North Atlantic (Conway and John, 2014), and quantitative trapping of this Zn in the  
181 strongly reducing sediment pile. The Peru upwelling region is micronutrient-limited (Fig.

182 DR1; e.g., Bruland et al., 2005). Such limitation is likely reflected in very low Zn  
183 concentrations in surface waters (indicating quantitative uptake). Furthermore, similar  
184 micronutrient-limited regions elsewhere in the ocean appear not to fractionate Zn  
185 isotopes (Zhao et al., 2014).

186 We calculate an average Pacific margin  $\delta^{66}\text{Zn}_{\text{auth}}$  composition weighted by  $\text{Zn}_{\text{XS}}$   
187 concentrations (Table DR2) and margin area (Table 1) of 0.12‰. If the Peru margin site  
188 is considered exceptional, and is excluded, this value decreases to  $-0.09\text{‰}$ . The global  
189 significance of this margin sink to oceanic mass balance depends on the magnitude of the  
190 Zn flux into margin sediments. Comparing the continental margin organic C deposition  
191 rate with the Zn/C ratio in plankton yields a preliminary flux estimate. Reported Zn/C  
192 ratios in phytoplankton vary widely (0.008 – 0.11 mmol Zn/ mol C: Twining and Baines,  
193 2013). The mean of compiled values is 0.036 mmol Zn/ mol C (Little et al., 2015).  
194 Jahnke (2010) estimates organic C deposition along the east pacific margins to be  $2.28 \times$   
195  $10^{12}$  mol/yr, and globally to be  $15.6 \times 10^{12}$  mol/yr. Taking these estimates at face value,  
196 we calculate a Pacific margin Zn deposition rate of  $0.8 \times 10^8$  mol/yr, and a global rate of  
197  $5.6 \times 10^8$  mol/yr. Such a flux would make margin sediments of equal or greater  
198 significance to the global oceanic mass balance compared to the oxic sink via sorption to  
199 Fe-Mn oxides, and is of the same order of magnitude as the projected missing Zn sink  
200 ( $\sim 3 \times 10^8$  mol/yr; Little et al., 2014). This approximation assumes that the Zn is solely  
201 supplied to sediment via cellular uptake, and that it is retained (e.g., in a sulfide phase) in  
202 the sediments following degradation of the organic matter. If some other means of Zn  
203 supply (e.g., direct diffusion from bottom waters, scavenging, or water column sulfide  
204 precipitation) is significant, then the sink may be larger. On the other hand, diffusion of

205 Zn back to the water column would reduce the flux magnitude. Nevertheless, to first  
206 order, the data presented in this study strongly support the hypothesis that modern  
207 continental margin sediments represent a significant isotopically light sink for Zn.

## 208 **CONCLUSIONS**

209 This study provides a means to explain the isotopically heavy Zn isotopic  
210 composition of seawater; that is, removal of light Zn isotopes to organic-rich continental  
211 margin sediments. In addition, we move a step closer to a quantitative understanding of  
212 the modern oceanic mass balance of Zn. A general framework can be envisaged whereby  
213 Zn is delivered to the deep ocean or sediment in organic matter, which may (or may not)  
214 be isotopically fractionated from the input value (typically of  $\sim 0.3\%$ ). Once in the  
215 reducing deep ocean or sediment, the Zn is sequestered in authigenic precipitates, either  
216 quantitatively, or partially. If sequestration is non-quantitative, there is potential for  
217 isotope fractionation, for example via precipitation of light Zn sulfides. Thus, it does not  
218 follow that the most sulfidic regime should necessarily exhibit the largest Zn isotope  
219 fractionation.

220 Isotopically heavy marine sediment Zn isotope ratios (Fig. 1) have previously  
221 been hypothesized to record biological processing in the surface ocean (e.g., Kunzmann  
222 et al., 2012). The implication of this study, supported by recent water column data and  
223 experimental studies (e.g., Bryan et al., 2014), is that this view may need to be revised.  
224 Instead, authigenic mineral formation in reducing environments may be the driver of the  
225 present-day heavy isotopic composition of seawater. Future studies should examine the  
226 transformation of biogenic Zn into more stable phases under different depositional redox  
227 conditions, both beneath highly productive margins and in locations with moderate to low

228 primary productivity, where anoxia is the result of restricted circulation (e.g., the Black  
229 Sea). Such studies will provide the basis for future application of Zn isotopes as a proxy  
230 for the past environment.

231

## 232 **ACKNOWLEDGMENT**

233 We thank three reviewers for comments that clarified our thinking, and improved  
234 the manuscript. Many thanks to Annie Hartwell for the carbon and sulfur analyses. This  
235 project work was supported by SNF - Project 200021\_153087 to DV. The University of  
236 Akron supported JM's participation in the project. A Leverhulme Trust Early Career  
237 Fellowship supports SL at Imperial College. Sample collection was supported by a  
238 number of NSF grants to JM, including OCE-0624777 and OCE-0219651. Gratitude is  
239 extended to colleagues William Berelson and Gary Klinkhammer for their contributions  
240 to cruises where some of these samples were collected.

## 241 **REFERENCES CITED**

- 242 Archer, C., and Vance, D., 2004, Mass discrimination correction in multiple-collector  
243 plasma source mass spectrometry: An example using Cu and Zn isotopes: *Journal of*  
244 *Analytical Atomic Spectrometry*, v. 19, p. 656–665, doi:10.1039/b315853e.
- 245 Bermin, J., Vance, D., Archer, C., and Statham, P.J., 2006, The determination of the  
246 isotopic composition of Cu and Zn in seawater: *Chemical Geology*, v. 226, p. 280–  
247 297, doi:10.1016/j.chemgeo.2005.09.025.
- 248 Bruland, K.W., Rue, E.L., Smith, G.J., and DiTullio, G.R., 2005, Iron, macronutrients  
249 and diatom blooms in the Peru upwelling regime: *Brown and blue waters of Peru:*  
250 *Marine Chemistry*, v. 93, p. 81–103, doi:10.1016/j.marchem.2004.06.011.

- 251 Bryan, A.L., Dong, S., Wilkes, E.B., and Wasylenki, L.E., 2015, Zinc isotope  
252 fractionation during adsorption onto Mn oxyhydroxide at low and high ionic  
253 strength: *Geochimica et Cosmochimica Acta*, v. 157, p. 182–197,  
254 doi:10.1016/j.gca.2015.01.026.
- 255 Chong, L.S., Prokopenko, M.G., Berelson, W.M., Townsend-Small, A., and McManus,  
256 J., 2012, Nitrogen cycling within suboxic and anoxic sediments from the continental  
257 margin of Western North America: *Marine Chemistry*, v. 128-129, p. 13–25,  
258 doi:10.1016/j.marchem.2011.10.007.
- 259 Conway, T.M., and John, S.G., Deutsch 2014, The biogeochemical cycling of zinc and  
260 zinc isotopes in the North Atlantic Ocean: *Global Biogeochemical Cycles*, v. 28,  
261 p. 1111–1128, doi:10.1002/2014GB004862.
- 262 Conway, T.M., and John, S.G., 2015, The cycling of iron, zinc and cadmium in the North  
263 East Pacific Ocean-insights from stable isotopes: *Geochimica et Cosmochimica*  
264 *Acta*, v. 164, p. 262–283, doi:10.1016/j.gca.2015.05.023.
- 265 Deutsch, C., et al., 2014, Centennial changes in North Pacific anoxia linked to tropical  
266 trade winds: *Science*, v. 345, p. 665–668, doi:10.1126/science.1252332.
- 267 Fujii, T., Moynier, F., Pons, M.L., and Albarède, F., 2011, The origin of Zn isotope  
268 fractionation in sulfides: *Geochimica et Cosmochimica Acta*, v. 75, p. 7632–7643,  
269 doi:10.1016/j.gca.2011.09.036.
- 270 Hartnett, H.E., Keil, R.G., Hedges, J.I., and Devol, A.H., 1998, Influence of oxygen  
271 exposure time on organic carbon preservation in continental margin sediments:  
272 *Nature*, v. 391, p. 572–575, doi:10.1038/35351.

- 273 Jahnke, R.A., 2010, Global Synthesis, *in* Liu, K.K., Atkinson, L., Quinones, R., and  
274 Talaue-McManus, L., eds., Carbon and nutrient fluxes in continental margins: A  
275 global synthesis: Springer-Verlag Berlin Heidelberg, p. 597–615, doi:10.1007/978-3-  
276 540-92735-8\_16.
- 277 Janssen, D.J., and Cullen, J.T., 2015, Decoupling of zinc and silicic acid in the subarctic  
278 northeast Pacific interior: *Marine Chemistry*, vol. 177, p. 124–133,  
279 doi:10.1016/j.marchem.2015.03.014.
- 280 John, S.G., and Conway, T.M., 2014, A role for scavenging in the marine biogeochemical  
281 cycling of zinc and zinc isotopes: *Earth and Planetary Science Letters*, v. 394, p.  
282 159–167.
- 283 John, S.G., Geis, R.W., Saito, M.A., and Boyle, E.A., 2007, Zinc isotope fractionation  
284 during high-affinity and low-affinity zinc transport by the marine diatom  
285 *Thalassiosira oceanica*: *Limnology and Oceanography*, v. 52, p. 2710–2714,  
286 doi:10.4319/lo.2007.52.6.2710.
- 287 Kunzmann, M., Halverson, G.P., Sossi, P.A., Raub, T.D., Payne, J.L., and Kirby, J.,  
288 2012, Zn isotope evidence for immediate resumption of primary productivity after  
289 snowball Earth: *Geology*, v. 41, p. 27–30, doi:10.1130/G33422.1.
- 290 Little, S.H., Vance, D., Walker-Brown, C., and Landing, W.M., 2014, The oceanic mass  
291 balance of copper and zinc isotopes, investigated by analysis of their inputs, and  
292 outputs to ferromanganese oxide sediments: *Geochimica et Cosmochimica Acta*,  
293 v. 125, p. 673–693, doi:10.1016/j.gca.2013.07.046.

- 294 Little, S.H., Vance, D., Lyons, T.W., and McManus, J., 2015, Controls on trace metal  
295 authigenic enrichment in reducing sediments: Insights from modern oxygen-deficient  
296 settings: *American Journal of Science*, v. 315, p. 77–119, doi:10.2475/02.2015.01.
- 297 McManus, J., Berelson, W.M., Severmann, S., Poulson, R.L., Hammond, D.E.,  
298 Klinkhammer, G.P., and Holm, C., 2006, Molybdenum and uranium geochemistry in  
299 continental margin sediments: Paleoproxy potential: *Geochimica et Cosmochimica*  
300 *Acta*, v. 70, p. 4643–4662, doi:10.1016/j.gca.2006.06.1564.
- 301 Morel, F.M.M., Reinfelder, J.R., Roberts, S.B., Chamberlain, C.P., Lee, J.G., and Yee,  
302 D., 1994, Zinc and carbon co-limitation of marine phytoplankton: *Nature*, v. 369,  
303 p. 740–742, doi:10.1038/369740a0
- 304 Roshan, S., and Wu, J., 2015, Water mass mixing is the dominant control on the zinc  
305 distribution in the North Atlantic Ocean: *Global Biogeochemical Cycles*, v. 29, p.  
306 1060–1074, doi:10.1002/2014GB005026
- 307 Rudnick, R.L., and Gao, S., 2003, Composition of the continental crust, *in* Rudnick, R.L.,  
308 ed., *The Crust, Volume 3, Treatise on Geochemistry*: Oxford, Elsevier-Pergamon, p.  
309 1–64.
- 310 SCOR Working Group, 2007, GEOTRACES—An international study of the global marine  
311 biogeochemical cycles of trace elements and their isotopes: *Chemie der Erde-*  
312 *Geochemistry*, v. 67, p. 85–131, doi:10.1016/j.chemer.2007.02.001.
- 313 Sinoir, M., Butler, E.C., Bowie, A.R., Mongin, M., Nesterenko, P.N., and Hassler, C.S.,  
314 2012, Zinc marine biogeochemistry in seawater: a review: *Marine & Freshwater*  
315 *Research*, v. 63, p. 644–657, doi:10.1071/MF11286.

- 316 Twining, B.S., and Baines, S.B., 2013, The Trace Metal Composition of Marine  
317 Phytoplankton: Annual Review of Marine Science, v. 5, p. 191–215,  
318 doi:10.1146/annurev-marine-121211-172322.
- 319 United States National Research Council, Institute of Medicine, 2000, Dietary Reference  
320 Intakes for Vitamin A, Vitamin K, Arsenic, Boron, Chromium, Copper, Iodine, Iron,  
321 Manganese, Molybdenum, Nickel, Silicon, Vanadium, and Zinc: Washington, D.C.,  
322 National Academies Press, p. 442–455.
- 323 Wedepohl, K.H., 1991, Chemical composition and fractionation of the continental crust:  
324 Geologische Rundschau, v. 80, p. 207–223, doi:10.1007/BF01829361.
- 325 Zhao, Y., Vance, D., Abouchami, W., and De Baar, H.J.W., 2014, Biogeochemical  
326 cycling of zinc and its isotopes in the Southern Ocean: *Geochimica et Cosmochimica*  
327 *Acta*, v. 125, p. 653–672, doi:10.1016/j.gca.2013.07.045.
- 328 Zheng, Y., Anderson, R.F., van Geen, A., and Kuwabara, J., 2000, Authigenic  
329 molybdenum formation in marine sediments: a link to pore water sulfide in the Santa  
330 Barbara Basin: *Geochimica et Cosmochimica Acta*, v. 64, p. 4165–4178,  
331 doi:10.1016/S0016-7037(00)00495-6.

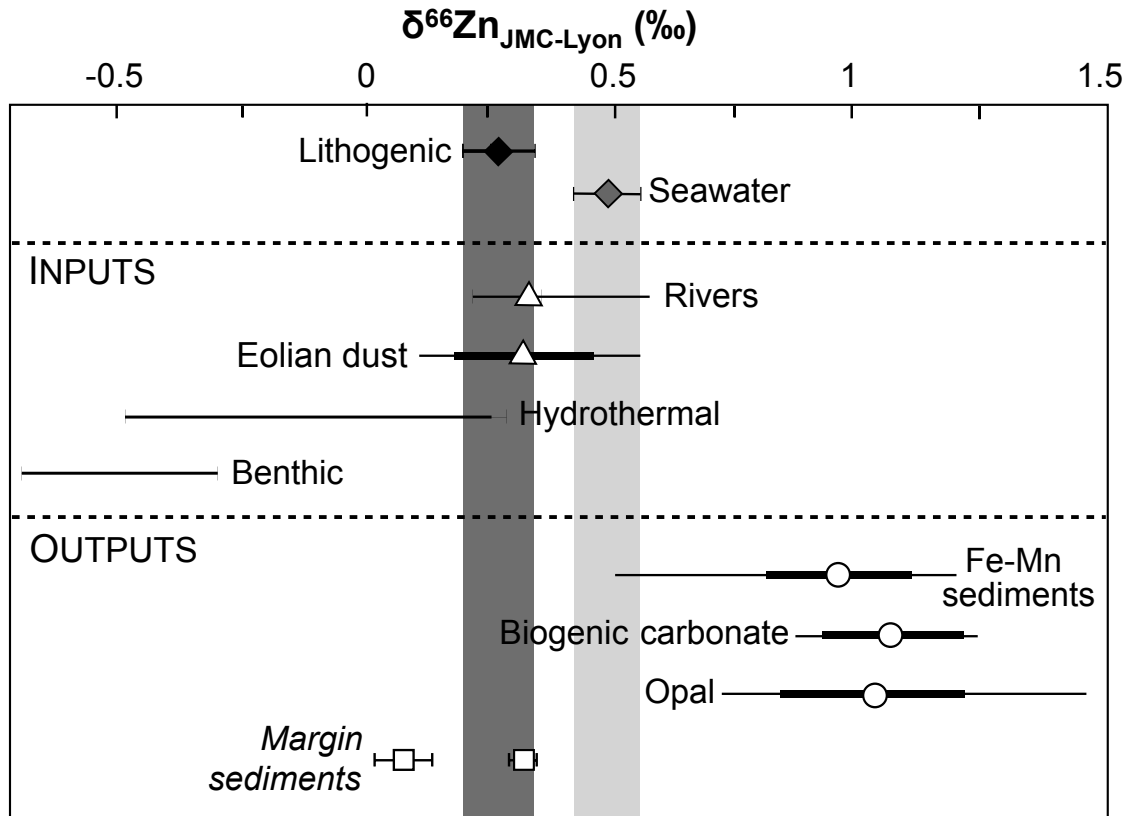
332

### 333 FIGURES

334 Figure 1. Range of compiled data sets (Table DR1) illustrating the natural variability in  
335  $\delta^{66}\text{Zn}$  in the marine realm, divided into the inputs to and outputs from the ocean. Where  
336 sufficient data exists, mean and 1SD are given as a symbol and thick black line. Shaded  
337 gray bars emphasize the respective isotopic compositions of the lithogenic and seawater



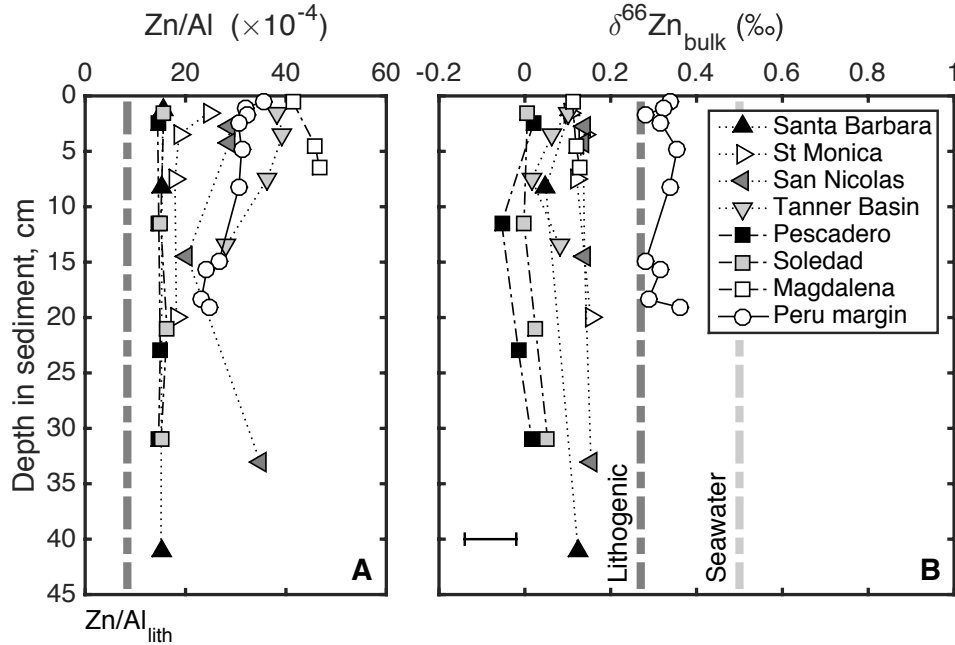
338 reservoirs. Mean and 1SD of measured bulk  $\delta^{66}\text{Zn}$  for margin sediments from this study  
339 are shown as two points, representing the Peru margin and all other sites.



340

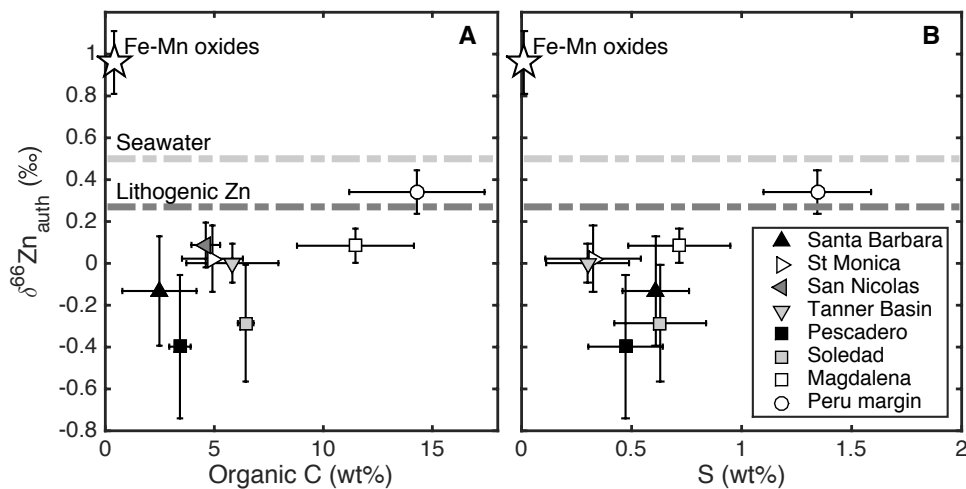
341

342 Figure 2. Down-core variability in (A)  $\text{Zn}/\text{Al}$  (by mass,  $\times 10^{-4}$ ) and (B)  $\delta^{66}\text{Zn}_{\text{bulk}}$  for the  
343 three continental margin locations (California Borderland basins: triangles; Mexican  
344 sites: squares; Peru margin: circles). 2-sigma uncertainty on isotope measurements  
345 ( $0.06\text{‰}$ ) is shown as a stand-alone error bar. Labeled gray-dashed vertical bars represent  
346 estimated  $(\text{Zn}/\text{Al})_{\text{lith}}$  and  $\delta^{66}\text{Zn}_{\text{lith}}$ , with average deep seawater  $\delta^{66}\text{Zn}$  for comparison.



347

348 Figure 3. a) Mean organic carbon (wt%) and b) Mean total S (wt%) versus mean  
 349 calculated  $\delta^{66}\text{Zn}_{\text{auth}}$  values for each site. Error bars on  $C_{\text{org}}$  and S values reflect the 2SD  
 350 for the whole sediment core, as thus reflect depth-dependent variation. Uncertainties on  
 351  $\delta^{66}\text{Zn}_{\text{auth}}$  are calculated via a Monte Carlo simulation carried out as described in the text.  
 352 For comparison, the mean and 1SD (Table DR1) of Fe-Mn oxide sediments are  
 353 represented by a star.



354

355

356 <sup>1</sup>GSA Data Repository item 2016xxx, xxxxxxxx, is available online at  
357 [www.geosociety.org/pubs/ft2015.htm](http://www.geosociety.org/pubs/ft2015.htm), or on request from [editing@geosociety.org](mailto:editing@geosociety.org) or  
358 Documents Secretary, GSA, P.O. Box 9140, Boulder, CO 80301, USA.

359

360

361

TABLE 1. SITE DESCRIPTIONS

Site	Latitude °N	Longitude °W	Margin area 10 <sup>6</sup> km <sup>2</sup>	Sediment core m	OMZ m	Sill depth m	Basin depth m	Bottom- water O <sub>2</sub> μM	Diagenetic class*	Sediment accumulation rate mg cm <sup>-2</sup> yr <sup>-1</sup>	Organic C burial flux mg cm <sup>-2</sup> yr <sup>-1</sup>	Refs
Peru Margin	-13.7	76.7	0.2	264	100–700	na	na	0–10	Ferr-Sulf	25	3.6 ± 0.4	1
Mexican Margin			0.1		500–1000							
Soledad Basin	25.2	112.7		544		250	545	0	Sulf	50–90	3.7 ± 0.1	1, 2, 3
Pescadero slope	24.3	108.2		616		na	na	0.4	Ferr	77	-	3
Magdalena	23.5	111.6		692		na	na	0.9	Ferr-Sulf	4–12	-	4
California Borderland Basins			0.1		200–1000							
Santa Barbara	34.3	120.0		493		475	600	0–10	Ferr-Sulf	92	-	5
Santa Monica	33.7	118.8		905		740	910	2–10	Ferr	16	0.7 ± 0.2	1
Tanner Basin	33.0	119.7		1514		1160	1550	~30	Mn-Ferr	12	0.8 ± 0.1	1
San Nicolas	32.8	118.8		1750		1100	1832	15–35	Mn	14	-	1

\*Diagenetic classifications are as follows: Sulf – sulfidic, Ferr – ferruginous, Mn – Mn-rich, sub-oxic.

1 McManus et al., 2006; 2 Chong et al., 2012; 3 Deutsch et al., 2014; 4 Hartnett et al., 1998; 5 Zheng et al., 2000

363

364

365